

1 **A comprehensive study of predicting turmeric yield using remote sensing and machine learning**  
2 **based models in the Lower Bhavani Basin, Tamilnadu, India**

3 **First Author**

4 Madhumitha Sathyamurthy,

5 Research Scholar, Institute of Remote Sensing, Anna University, Chennai, India - 600025

6 [madhumitha2599@gmail.com](mailto:madhumitha2599@gmail.com)

7 **Second Author**

8 Dr Murugasan Rajiah,

9 Professor, Institute of Remote Sensing, Anna University, Chennai, India – 600025

10 [murugasanr@rediffmail.com](mailto:murugasanr@rediffmail.com)

11 **Third Author**

12 Dr. Saravanan Ramasamy,

13 Professor, Centre for Water Resources, Anna University, Chennai, India – 600025

14 [rsarancwr@gmail.com](mailto:rsarancwr@gmail.com)

15 **Fourth Author**

16 Dr. Shanmugam Madhavan,

17 Associate Professor, Institute of Remote Sensing, Anna University, Chennai, India – 600025

18 [shan\\_mc50@yahoo.com](mailto:shan_mc50@yahoo.com)

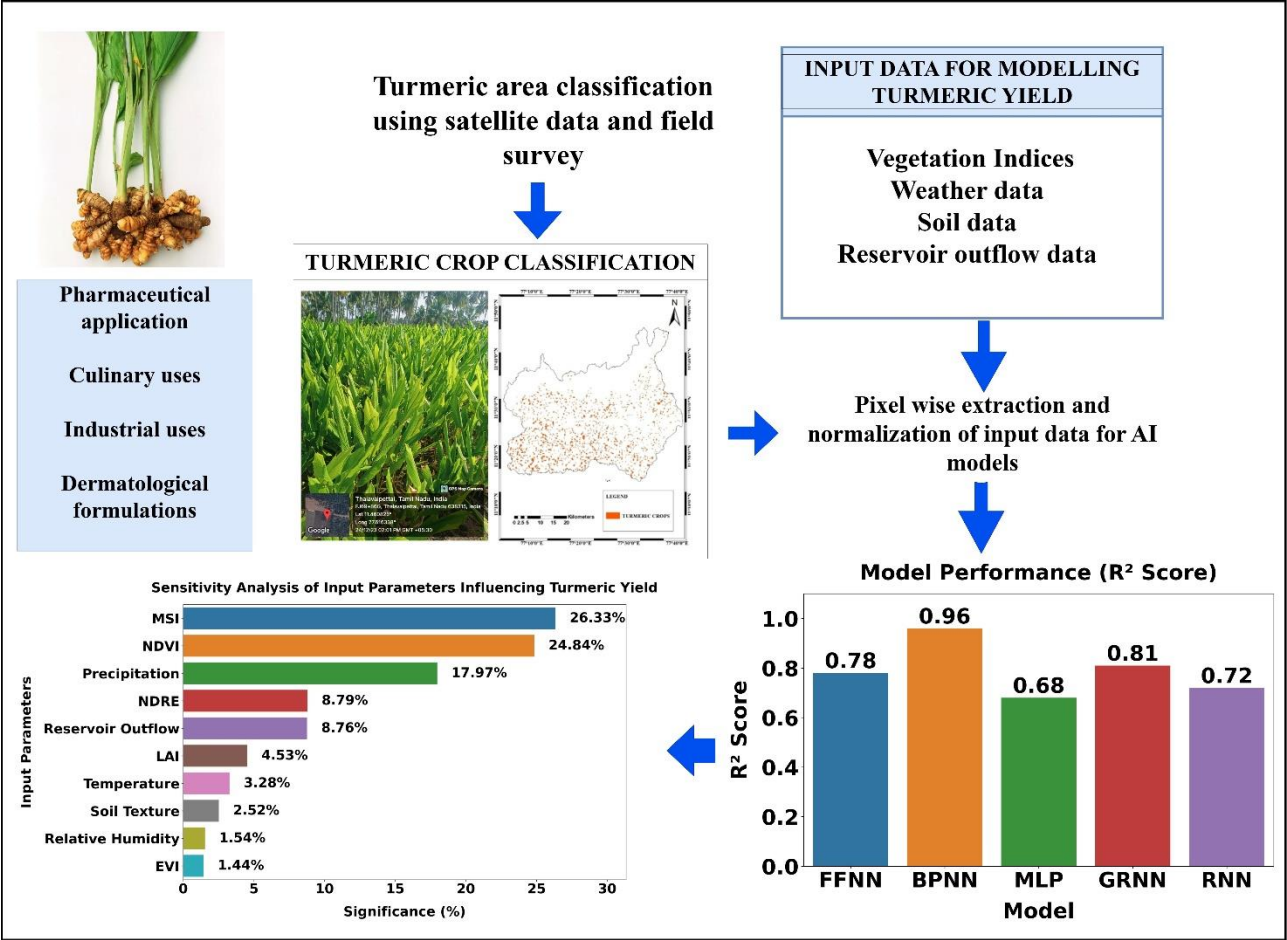
19 **Corresponding Author**

20 Madhumitha Sathyamurthy

21 Research Scholar, Institute of Remote Sensing, CEG, Anna University, Chennai, India – 600025.

22 Phone number: 7373776777

23 [madhumitha2599@gmail.com](mailto:madhumitha2599@gmail.com)



25

26

27

28

29

30

31

32

33

34

## 35 Abstract

36 Crop yield forecasting is an essential element for farm management directly impacting food  
37 security, economic planning and sustainability of resources. This study integrated remote sensing data  
38 and machine learning approaches to develop an advanced turmeric yield modelling framework for  
39 turmeric crops grown in the study area. The input parameters included vegetation indices, soil texture  
40 and meteorological and hydrological variables. The findings showed that the Back Propagation  
41 Neural Network (BPNN) model ( $R^2 = 0.96$ ) outperformed other models utilized in this study in  
42 predicting turmeric yield. Sensitivity analysis further highlighted that the turmeric yield was highly  
43 sensitive to the Normalized Difference Vegetation Index (NDVI), Moisture Stress Index (MSI) and  
44 precipitation. This modelling approach provided a reliable tool for early yield estimation at the  
45 maturity phase with a 0.86 % deviation from the actual turmeric yield, aiding farmers and  
46 policymakers in optimising crop management practices and enhancing decision-making processes.  
47 This study presented a holistic approach for scalable data-driven agricultural innovation contributing  
48 to efficient and sustainable crop production systems.

49 **Keywords:** Crop yield, Turmeric, Remote Sensing, Vegetation Indices, Machine learning

## 51 1. Introduction

52 Crop yield reflects agricultural productivity and is directly related to food security, the income  
53 and economic well-being of farmers. Crop production forecasts based on weather conditions will  
54 help farmers, policymakers and administrators in coping with adversity (Das *et al.* 2018). Crop  
55 yield models which provide timely and accurate yield estimates using satellite data and advanced  
56 analytics, play a key role in agricultural insurance by supporting risk assessment, policy  
57 formulation and claim management (Mateo-Sanchis *et al.* 2020; Mena *et al.* 2024; Rojas *et al.*  
58 2011).

Crop yield was forecasted by using traditional models based on soil characteristics and climatic factors utilising simple and multiple linear regression models (Abrougui *et al.* 2019). A model such as SPUDSIM was limited to predict the potato yield at the state level (Resop *et al.* 2012). Crop models demand extensive input parameters including soil properties, weather parameters and yield variables for validation and assessment, as they replicate crop growth regularly (Ahmad *et al.* 2018). Remote sensing technology offers crop information, environmental conditions and land management. MODIS-derived vegetation indices such as NDVI, Enhanced Vegetation Index (EVI), Land Surface Temperature (LST), Leaf Area Index (LAI) and Vegetation Condition Index (VCI) were employed for crop yield estimation (Ronchetti *et al.* 2023; Potopova *et al.* 2020; Johnson. 2014; Setiyono *et al.*, 2018). Sentinel 2-derived indices like NDVI, Red Edge NDVI, Chlorophyll Index Red Edge (CIRED) and Canopy Chlorophyll Content were employed in the construction of crop yield models (Hunt *et al.* 2019; Schwalbert *et al.* 2018; Dimov *et al.* 2022; Hara *et al.* 2021). Crop yield at maturity stages had the greatest precision in comparison with other crop developmental stages (Amankulova *et al.* 2023; Nevavuori *et al.* 2019; Tedesco *et al.* 2021; Zhou *et al.* 2017). Most of the studies considered either vegetation indices such as NDVI and EVI or environmental factors (e.g., precipitation, temperature) and rarely combined both data types for holistic modelling (Muruganantham *et al.* 2022). The literature review emphasized that multisource data fusion can enhance prediction accuracy but is underutilized for underrepresented crops such as turmeric (Joshi *et al.* 2023). This study offered a comprehensive modelling strategy that addresses this gap directly by integrating Sentinel-2 indices (NDVI, EVI, LAI, MSI, NDRE) with real-time precipitation, temperature, relative humidity and reservoir outflow. While Sentinel-2 data are universal in applications to common crops, their utilization for turmeric, particularly by employing several indices was limited. This study employed such indices to forecast turmeric yield and opened up new fronts in Sentinel data-specific crop applications.

The Feed Forward Neural Network (FFNN) model was built to forecast maize yield in Kenya based on precipitation, temperature, evapotranspiration, soil moisture and Landsat 7 NDVI (Mwaura & Kenduiywo, 2021). Generalized Regression Neural Network (GRNN) models were employed to simulate paddy yield with enhanced precision (Joshua *et al.* 2021). BPNN models simulated winter wheat yield more accurately at the field scale level (Tang *et al.* 2022). Convolutional Neural Network (CNN) and Long Short Term Memory (LSTM) models were employed in constructing crop yield models (Sun *et al.* 2019). RNN models efficiently captured temporal relationships and were best suited for accurate time-series-based crop yield prediction (Bali & Singla. 2021). Research showed that the MLP model enhanced crop yield prediction accuracy from crop phenology (Yesilkoy & Demir. 2024). An Artificial Neural Network (ANN) model was introduced for curcumin content estimation based on soil, climate parameters, pH and organic carbon with  $R^2 = 0.91$  (Akbar *et al.* 2016). A model of yield prediction of turmeric was established through the application of ANN employing soil and climatic parameters as the input variables and estimated the yield as  $R = 0.88$  (Akbar *et al.* 2018). Machine learning models were applied to analyze the yield trend of turmeric employing rainfall, temperature, soil moisture, pH value and mean wind speed to predict yields. The predictive models employed were RNN, LSTM, BPNN and Gated Recurrent Unit (GRU). For predicting turmeric yield, GRU performed better than the other algorithms (Raju *et al.* 2023). A hybrid method integrating deep learning and remote sensing data assimilation (Temporal Fusion Transformer) was created to make interactive wheat breeding yield prediction possible (Yang *et al.*, 2025). A hybrid CNN-LSTM with skip connections and attention-based mechanisms was used to make high-accuracy predictions of wheat and rice yields in India (Dharwadkar *et al.*, 2023). The Multi-Modal Spatial-Temporal Vision Transformer (MMST-ViT) employed remote sensing images and meteorological data to enhance yield prediction (Lin *et al.*, 2023). Deep Learning architectures have been widely employed for predicting yields. This research although concentrating on a traditional method

provides a baseline for future incorporation of sophisticated deep learning methods designed for crop-specific use like that of turmeric. Nonetheless, the effectiveness of deep learning models frequently relies on the availability of large, high-quality datasets and substantial computational resources. This research employed a suite of models chosen for their trade-off between model complexity, performance and interpretability. They are particularly well-adapted to structured, medium-sized datasets where overfitting is a problem and interpretability is critical to agricultural decision-making.

While machine learning methods had been used in other crops, the application of turmeric had been minimal using sophisticated neural networks like FFNN, BPNN, MLP, GRNN and RNN. The effective use of sophisticated machine learning techniques in overall agriculture has been studied but it was noted that they can only be used in crops such as turmeric (Aslan *et al.* 2024). Research indicated that the joint application of remote sensing and ANN was a useful instrument in crop yield estimation (Bassine *et al.* 2023; Bharadiya *et al.* 2023; Huber *et al.* 2024; Kavipriya and Vadivu, 2024; Khaki and Wang, 2019; Sajid *et al.* 2022). The models utilized in this research were constructed with great consideration of hyperparameter tuning in order to maximize performance, with hyperparameters including the number of hidden layers, neurons per layer, learning rate, activation functions and batch size systematically experimented and tested. The FFNN architecture consisted of 10 hidden layers, chosen based on preliminary experiments aimed at balancing model depth with overfitting risk, consistent with similar applications in crop yield prediction (Singh *et al.* 2023). An L2 regularization parameter ( $\lambda = 0.0001$ ) was applied to reduce overfitting by penalizing large weights (Goodfellow *et al.* 2016). A dropout rate of 20% was introduced between layers to further prevent overfitting by randomly deactivating neurons during training, aligning with best practices suggested in deep learning literature (Srivastava *et al.* 2014). The hyperparameters were either empirically chosen from repeated trials or tuned through trial-

and-error and performance measures to ensure model stability at the cost of interpretability important for real-world agricultural applications.

More recent studies have become more concerned with assessing climate change impacts on agriculture based on the Shared Socioeconomic Pathway (SSP) scenario, which prescribes various socio-economic development paths and corresponding greenhouse gas emissions. Climate impacts on rice yield under SSP1-2.6, SSP2-4.5, SSP3-7.0 and SSP5-8.5 were projected based on Coupled Model Intercomparison Project (CMIP6) models. Findings revealed that rice yield may increase in lower emissions up to the middle of this century, with subsequent stabilization (Xu *et al.*, 2024). Climate change impacts on crop yield anomalies were examined in the SSP scenario. The research estimated elevated heat and drought stress with higher frequency yield losses, particularly for wheat (Schmidt & Felsche, 2024). Such research underscores the need to include SSP scenarios in crop modelling in order to comprehend potential future issues better and guide policy decisions.

Recent developments in underground crop remote sensing have opened new possibilities for enhancing yield prediction accuracy by incorporating subsurface biophysical parameters. Techniques such as root zone moisture estimation, soil nutrient mapping through proximal spectroscopy and subsurface structure assessment using microwave and Ground Penetrating Radar (GPR) have demonstrated strong potential in early stress detection and soil-plant interaction modelling (Bulacio Fischer *et al.* 2025; Li *et al.* 2023). Although the present study primarily employed above-ground spectral indices and climatic inputs, future model extensions may benefit from integrating these underground sensing modalities to capture below-surface dynamics affecting turmeric growth, especially under climate-induced stress conditions. Turmeric yield estimation is especially challenging since it relies on underground biomass (rhizomes), which is hard to estimate using conventional remote sensing techniques. Crop yield research indicated that combining spectral indices with environmental factors can enhance predictions for underground crops but recognizes that this continues to be an

enormous challenge (Ishaq *et al.* 2024). This study bridges the gap by merging Sentinel-2 indices with climatic and hydrological information, which could correlate surface conditions with subterranean biomass growth. This study employed remote sensing variables, machine learning models and environmental traits to construct a valid model for forecasting turmeric yield. Remote sensing facilitates the extraction of phenological crop data (Ji *et al.* 2021). This fusion poses notable challenges, including differences in spatial and temporal resolution, variable data quality and the need for normalization across disparate sources. Such challenges are rarely addressed in prior studies, which often focus on above-ground crops like wheat, rice, or maize that show clearer spectral signals. Unlike models tailored for crops with visible yield indicators, this approach is structured to capture subtle variations in biophysical and environmental parameters that indirectly influence underground biomass. This positions the study as a novel contribution to the field, both in terms of methodology and its application to traditionally underrepresented crop types. This research examined all phases of plant growth and paved the way for prediction at an early stage. Contributing to the debate on relationships between climate parameters, soil condition and vegetation indices, this research facilitates future research in sustainable agriculture and the environmental context. The research objectives are listed below.

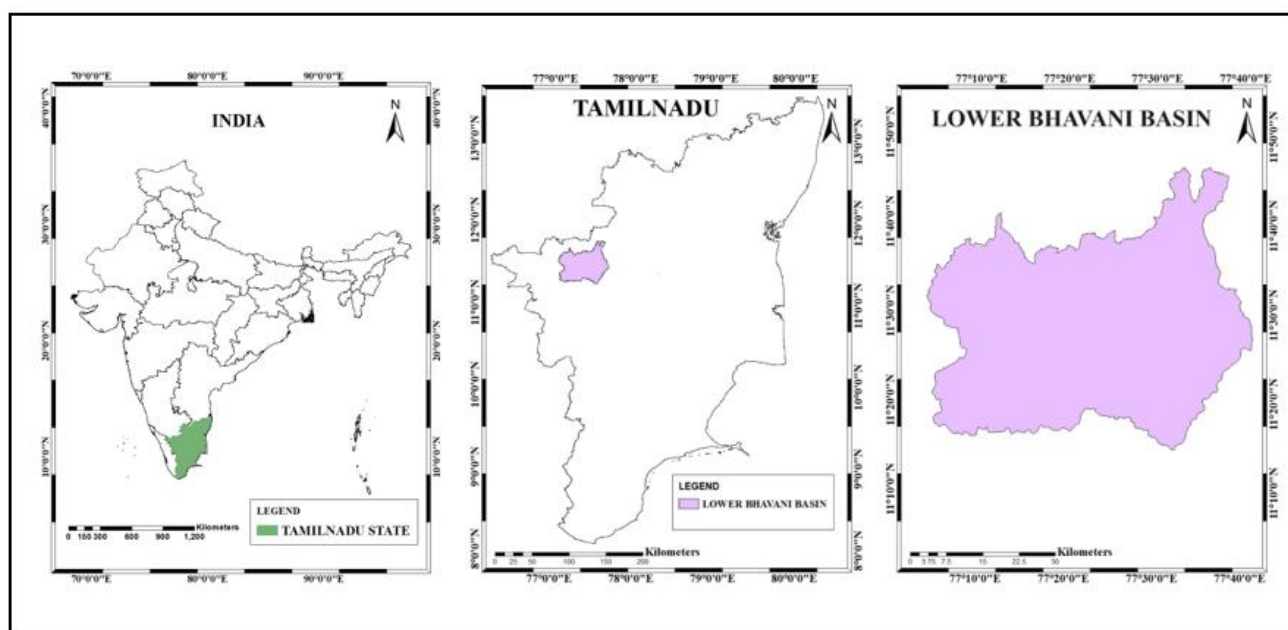
- i. To carry out a correlation analysis between the input variables and turmeric yield.
- ii. To develop machine learning-based turmeric yield models (FFNN, BPNN, GRNN, MLP and RNN).
- iii. To examine the sensitivity of the input variables in influencing the turmeric yield.
- iv. To assess the model's predictive ability in forecasting turmeric yield at each growth stage.



## 186 2. Materials and Methods

### 187 2.1 Study Area

188 The study area, Lower Bhavani Basin is the sub-basin of the Cauvery Basin in Tamil  
189 Nadu, India. It comprises parts of Erode, Coimbatore and Tiruppur districts. The area of this  
190 basin is 2424 Km<sup>2</sup>. Bhavani River, a tributary of the Cauvery River, flows in this basin and  
191 acts as a source of irrigation. The average rainfall in this basin is 130 mm. The temperature  
192 ranges from 22 to 38°C. The average relative humidity of this area ranges from 65 – 95 %.  
193 About 59 % of the geographical area of the study area is subjected to agricultural practice. The  
194 major crops grown in the basin are turmeric, sugarcane, banana, groundnut and paddy. The  
195 crop chosen for this study is turmeric. Turmeric crops are grown in an area of 4694.82 ha. The  
196 study area map is shown in **Error! Reference source not found..**



198  
199 Figure 1 Study area map  
200  
201  
202

## 203 2.2 Methodology

204 The non-spatial datasets such as precipitation, temperature, relative humidity, soil  
205 texture, reservoir outflow and turmeric yield data were obtained from the local administration  
206 department of the study area. Precipitation during the cropping period ranged from 0 mm to 470  
207 mm per month (mean = 212 mm; Standard Deviation (SD) = 96 mm), reflecting seasonal  
208 variability. Monthly average temperature ranged from 18°C to 32°C (mean = 26.4°C; SD =  
209 3.1°C). Relative humidity varied between 53% and 95% (mean = 78.6%; SD = 9.2%), indicating  
210 a wide range of atmospheric moisture conditions. Reservoir outflow ranged from 60,000 to  
211 80,000 cusecs (mean = 71,400 cusecs; SD = 5,700 cusecs), ensuring continuous irrigation  
212 availability. Soil texture data were obtained from the regional Agricultural Department, which  
213 classifies soil types based on the United States Department of Agriculture (USDA) soil texture  
214 classification system. Based on the proportions of sand, silt and clay, samples were categorized  
215 into four predominant texture classes Sandy, Loamy Sand, Sandy Loam and Clay Loam. The  
216 spatial dataset such as vegetation indices (NDVI, EVI, LAI, MSI and NDRE) were extracted  
217 from the optical dataset of Sentinel 2 level 1C imagery using band math in ArcGIS.  
218 Preprocessing of the imagery was done employing the Sentinel Application Platform (SNAP)  
219 software. Radiometric Correction involved converting Level-1C Top Of Atmosphere reflectance  
220 to surface reflectance using the Sen2Cor processor within SNAP. Atmospheric Correction was  
221 performed using the Scene Classification and aerosol correction modules in Sen2Cor. Cloud  
222 mask was applied using the Scene Classification Layer band to eliminate invalid pixels.  
223 Including parameters such as vegetation indices, soil and climate data ensures an extensive  
224 modelling approach that reflects real-world environmental interconnections. The use of field-  
225 derived and remotely sensed parameters enhances the relevance and applicability of the findings.  
226 The bands in the spatial dataset had been resampled to 10 m spatial resolution. The spatial and  
227 non-spatial data were collected for the period 2016 to 2022. Land Use Land Cover (LULC) maps  
228 were prepared from field survey and Sentinel 2 imagery using a Maximum Likelihood Classifier

(MLC). The turmeric areas were spatially extracted from the LULC map. The non-spatial precipitation dataset was interpolated as spatial maps using the kriging interpolation technique. The categorical values of soil texture data were pre-processed using one hot encoding technique. These were encoded into binary vectors [0, 1] for each class using the `get_dummies()` function in Python, allowing the model to interpret soil types as separate input features. A correlation analysis was carried out between the input variables and turmeric yield. The FFNN, BPNN, MLP, GRNN and RNN models were developed to forecast turmeric yield using MATLAB by training with the input variables. A sensitivity analysis between the input variables and the crop yield results was carried out. Future turmeric yield prediction was done with the best model developed in this study. To assess the long-term impact of climate change on the turmeric yield model was trained using historical yield and climate data. The model was used to simulate yield projections up to the year 2100. Future precipitation projections were sourced from the CMIP6 dataset under five Shared Socioeconomic Pathways (SSPs) which include SSP1-2.6, SSP2-4.5, SSP3-7.0, SSP4-6.0 and SSP5-8.5. Bias-corrected annual precipitation values from each SSP were used as input into the trained model to simulate the future turmeric yield. The precision of the model in determining the yield at every crop growth stage is analysed.

### **3. Results and discussion**

#### **3.1 Spatial delineation of crop area**

To focus on agricultural crop yield prediction, the crop land was extracted by masking out non-agricultural areas. This ensures that only relevant regions were retained for further classification. Using training samples collected from ground truth data, spectral signatures were analysed to classify turmeric cultivation areas. The classification successfully differentiated turmeric fields based on their spectral reflectance patterns in satellite imagery. The final classified map displayed turmeric cultivation areas distinctly, providing a spatial representation of their distribution. This classification served as a crucial input for subsequent yield prediction modelling

and analysis. The map showing turmeric regions in the study area is shown in **Error! Reference source not found..**

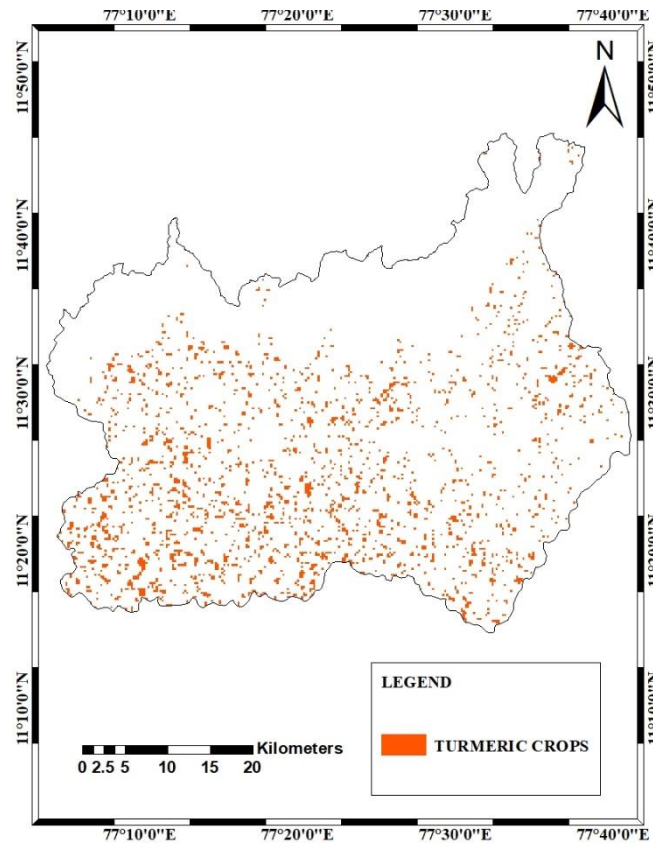


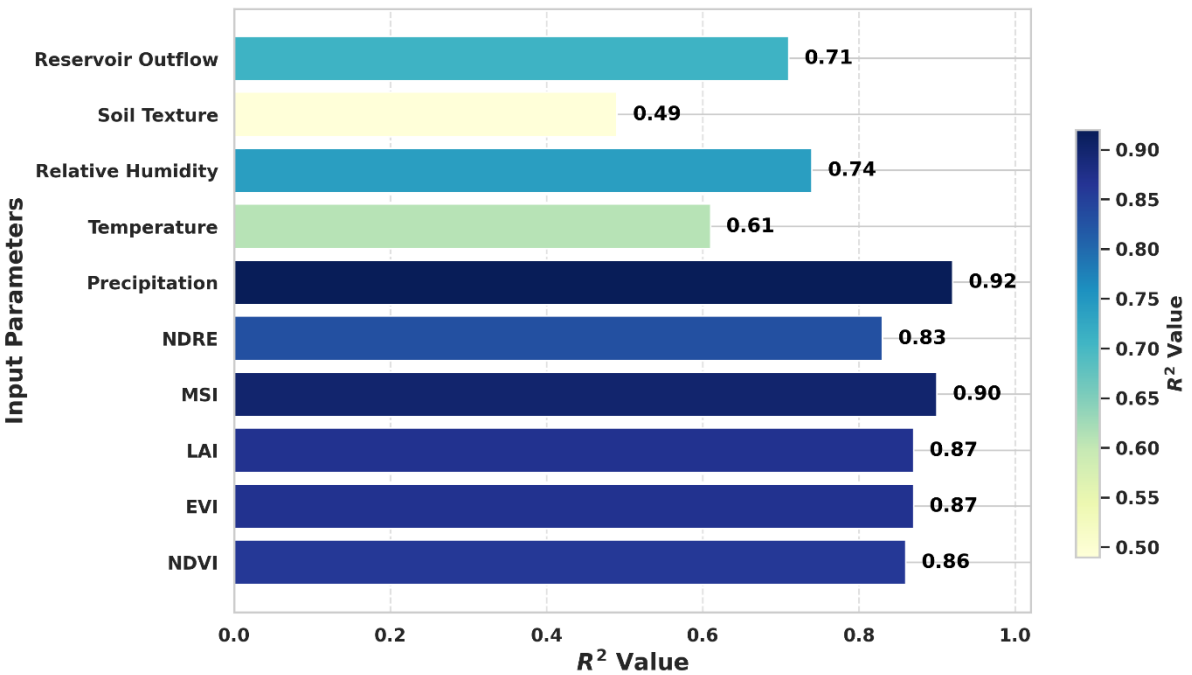
**Figure 2 Map showing turmeric regions in the study area**

**3.2 Analysis of the accuracy assessment results**

The accuracy assessment of the classification further validated the effectiveness of the approach in mapping crop-specific land cover. The classified output was validated using the kappa coefficient, which quantifies classification agreement beyond chance. Overall accuracy indicated that 91.67% of the classified pixels match the reference data, demonstrating a high accuracy in the classification. The Kappa Coefficient was approximately 0.90, indicating almost perfect agreement in classification. The Turmeric classes were classified with 100% accuracy, confirming that their spectral signatures were distinct and that their areas did not overlap significantly.

269     **3.3 Correlation Analysis**

270             The correlation analysis results of turmeric yield with input parameters are shown in  
271     **Error! Reference source not found..** Adequate precipitation ensured the plant received enough  
272     water, leading to healthy growth and higher yields and had a very strong correlation with turmeric  
273     yield with  $R^2 = 0.92$ . A higher MSI in the study area, indicating lower water stress, correlated  
274     strongly with better turmeric yields ( $R^2 = 0.90$ ) since the crop was sensitive to moisture  
275     availability. NDVI ( $R^2 = 0.86$ ), EVI ( $R^2 = 0.87$ ), LAI ( $R^2 = 0.87$ ) and NDRE ( $R^2 = 0.83$ ) had a  
276     strong correlation with turmeric yield as the plant benefits from a healthy and dense canopy, which  
277     supported better photosynthesis and ultimately higher yields.



279             **Figure 3 Correlation analysis between input parameters and turmeric yield**

282             High relative humidity reduces water loss through evapotranspiration, maintains  
283     moisture levels and promotes better growth in the turmeric plants and had a strong correlation  
284

with turmeric yield with  $R^2 = 0.74$ . Reservoir outflow influences irrigation water availability and was strongly correlated with turmeric yield with  $R^2 = 0.71$ . Turmeric can tolerate a range of temperatures and there is an optimal range that promotes maximum growth and yield, leading to this moderate correlation ( $R^2 = 0.61$ ). The influence of soil texture on turmeric yield was less and had a moderate correlation with  $R^2 = 0.49$ . These key trends demonstrated that water-related parameters, both direct (rainfall) and indirect (MSI, RH, reservoir outflow) were dominant drivers of turmeric yield in the study area. Vegetation indices were closely clustered suggesting that canopy health and density are consistently strong predictors of yield. Climatic and vegetation indices outperformed temperature and soil texture implying soil texture was less limiting in the region, or may not vary much. The combination of rainfall, vegetation vigour and irrigation (reservoir outflow) indicated a synergistic effect, where both natural and managed water sources support yield.

### 3.4 Turmeric yield models

This study developed FFNN, BPNN, MLP, GRNN and RNN to predict turmeric yield in the study area. All the models were trained and validated using a systematic data split, with 70% of the dataset used for training, 15% for validation and 15% for testing to ensure robust evaluation and prevent overfitting. Hyperparameters for each model were selected based on both empirical tuning and literature support, ensuring a balance between model complexity and generalizability. To ensure consistency and comparability across the multisource input variables, all input features were normalized using Min-Max scaling to a range between 0 and 1. This normalization process is particularly important when integrating variables with differing units and magnitudes, such as vegetation indices (NDVI, EVI, NDRE, MSI, LAI), climatic variables (rainfall, temperature, relative humidity), reservoir outflow, and soil texture. This step mitigates the influence of varying scales, ensures equal contribution of all features during model training, and enhances model convergence and stability. Normalization was applied prior to data partitioning to prevent data

leakage. After training and tuning with a 70:15:15 split (training: validation: test), each model's final performance was evaluated on the test data. The performance metrics listed in **Error! Reference source not found.** represent the validation results used to compare model accuracy and generalization ability.

#### a. FFNN

The FFNN model had an  $R^2$  value of 0.78. The number of hidden layers for this FFNN model was 10. The FFNN model was trained using the Adam optimizer, a learning rate of 0.001 and a batch size of 32. The ReLU activation function was applied to each hidden layer. The FFNN model was trained with a learning rate of 0.001 and batch size of 32. The ReLU activation function was applied to each hidden layer and the model was trained over 100 epochs using Mean Squared Error (MSE) as the loss function. Each hidden layer captured and refined features from the input data, resulting in an improved comprehension of the variables that affect turmeric yield.

#### b. BPNN

The BPNN model produced an  $R^2$  value of 0.96. The model had 10 hidden layers and was trained for 100 epochs. A batch size of 32 was chosen for effective training. L2 regularization ( $\lambda = 0.0001$ ) was used to avoid overfitting. The dropout rate was chosen as 20% to enhance generalization. The backpropagation algorithm updated model weights repeatedly, optimizing feature relationships for enhanced prediction accuracy. This stratification preserved class balance and avoided temporal leakage. The model's performance was assessed not only on the test set but also across 10 repeated runs with different random seeds to evaluate generalization.

### c. MLP

The MLP model had an  $R^2$  value of 0.68. The training was done with 10 hidden layers and 100 epochs, employing the Stochastic Gradient Descent (SGD) optimizer with a momentum value of 0.9. The learning rate was 0.01 and the batch size was 64 for stable training. ReLU activation was used in hidden layers and dropout (15%) was added.

### d. GRNN

The GRNN model provided an  $R^2$  value of 0.81. The model utilized a radial basis function (Gaussian kernel) with the smoothing factor fixed at 0.1 to regulate the bias-variance trade-off. The batch size was 64 and early stopping was performed using a 15% validation set. Hyperparameters tuned included learning rate (0.1), momentum (0.99), dropout (15%) and batch size (64).

### e. RNN

The RNN model generated an  $R^2$  of 0.72. The model was trained on 10 hidden layers and 100 epochs with the Adam optimizer with a learning rate of 0.001. The batch size was set to 32 for computational efficiency. Gradient clipping (max norm = 5) was implemented to avoid exploding gradients. 25% dropout was used to enhance generalization. Temporal dependencies were explicitly captured by structuring the input data as time-series sequences across multiple crop growth stages from 2016 to 2022. For the RNN model, time-dependent features such as vegetation indices and weather variables were organized into sequential input windows representing monthly intervals throughout the growing season. This allowed the model to learn temporal dynamics in crop development and environmental variability. Each input sequence was associated with a corresponding yield label, enabling supervised learning over temporal patterns. Padding and masking techniques were not required, as sequence



lengths were consistent across samples. Hyperparameters for the RNN were selected based on grid search and manual tuning. The Adam optimizer was used due to its efficiency in handling sparse gradients. These tuning processes were validated using k-fold cross-validation and a hold-out validation set, ensuring that parameter choices enhanced temporal pattern learning while minimizing overfitting.

Of the models that were trained for predicting turmeric yield, BPNN showed the best accuracy with an  $R^2$  value of 0.96. The GRNN, FFNN, MLP and RNN had moderate prediction performance, with GRNN using a non-iterative technique and a radial basis function to produce a localized estimation of yield. The RNN model used recurrent connections to capture temporal dependencies. Overall, BPNN emerged as the most successful model and was considered for further analysis to improve its accuracy and robustness for predicting turmeric yield.

**Table 1 Validation metrics of the turmeric yield models**

Model	$R^2$	RMSE (t ha <sup>-1</sup> )	MSE (t ha <sup>-1</sup> )	MAE (t ha <sup>-1</sup> )
FFNN	0.78	3.92	15.37	5.78
BPNN	0.96	0.22	0.05	1.04
MLP	0.68	4.78	22.85	7.32
GRNN	0.81	5.23	27.37	8.45
RNN	0.72	6.10	37.21	9.80

In comparison with previous literature, the present study's BPNN model, which had an  $R^2$  of 0.96, performed much better than the  $R^2$  of 0.80 in earlier research, indicating the improved capability of the proposed model to identify intricate nonlinear interactions for precise turmeric yield prediction (Tang *et al.* 2022). The  $R^2$  of 0.81 achieved by the GRNN model in this research is slightly lower than the  $R^2$  of 0.90 discussed in previous studies but still within a similar range and may differ due to variations in crop type, spatial scale, or input diversity of the model (Joshua *et al.* 2021). The FFNN model yielded an  $R^2$  of 0.78, which was in close agreement with the  $R^2$  of 0.64 reported in similar studies, indicating consistent performance on different datasets and environmental settings (Mwaura & Kenduiywo, 2021). Likewise, the MLP model had an  $R^2$  of 0.68, significantly greater than the 0.37 reported elsewhere, reflecting improved generalization and stability of the current model despite differences in architecture and data properties (El-Kenawy *et al.* 2025). The RNN model had an  $R^2$  value of 0.72, very similar to the  $R^2$  value of 0.75 from existing research, confirming recurrent architectures' success in modelling temporal relationships for crop yield prediction (Bali & Singla. 2021). In general, the results of this study show not only consistency with prior research but also enhanced prediction performance, especially for the BPNN model, thus justifying the methodological decisions and reliability of the implemented framework.

The Table **Error! Reference source not found.** presents the mean  $R^2$ , standard deviation and 95% confidence intervals (CI) for each model across 10 trials to assess if the performance differences are statistically significant.

**Table 2 Summary of Model Performance with Statistical Significance**

Model	Mean R <sup>2</sup>	Standard Deviation	95 % CI Lower	95 % CI Upper
BPNN	0.9462	0.0071	0.9417	0.9506
FFNN	0.7786	0.0064	0.7746	0.7826
MLP	0.6775	0.0118	0.6702	0.6849
GRNN	0.8085	0.0067	0.8043	0.8126
RNN	0.7152	0.0081	0.7101	0.7202

The very low p-value =  $3.2 \times 10^{-16}$  ( $< 0.05$ ) calculated from the ANOVA test indicated a statistically significant difference in mean R<sup>2</sup> values among the five models. BPNN outperformed all other models significantly, with a narrow confidence interval, suggesting high stability and low sensitivity to random initialization. MLP showed the lowest predictive power and the widest interval, indicating comparatively poor and less stable performance. The differences between intermediate-performing models (FFNN, GRNN, RNN) are also significant due to the overall low variance and tight intervals.

### 3.5 Sensitivity analysis

Sensitivity analysis determined the elements that most significantly affect crop yield. The One AT a Time (OAT) sensitivity analysis has been performed and the results are shown in **Error! Reference source not found..** The results showed that MSI, NDVI and precipitation significantly impacted turmeric yield since these factors have a direct impact on plant health, water availability and soil fertility. MSI was the most important parameter having maximum sensitivity. Maximum sensitivity could be attributed to the biological nature of turmeric. Turmeric is a water-requiring crop and the growth of rhizomes is most sensitive to moisture

stress. MSI is an index of plant water stress. High MSI indicates water-deficient conditions, which affect photosynthesis and rhizome growth and consequently reduce yield. The rhizome, as the economic yield fraction of turmeric, is particularly sensitive during water-sensitive growth phases like sprouting and bulking. Therefore, even limited water stress during these growth phases can significantly influence the final yield. Hence, such an intimate relationship between plant water status and turmeric productivity is suitably depicted by the dominant role of MSI in the model. This high reliance supports the agronomic observation that ensuring proper irrigation and reducing drought stress is vital to maximize turmeric yield and implies that MSI can be used as a surrogate for crop health monitoring and irrigation scheduling in turmeric production systems. NDRE and reservoir outflow had a moderate impact on turmeric yield. LAI, temperature, relative humidity and EVI had a lower impact on yield because turmeric was less sensitive to minor variations in these parameters. The significance of input variables in decreasing order were MSI, NDVI, precipitation, NDRE, reservoir outflow, LAI, temperature, soil texture, relative humidity and EVI. The significance levels of MSI, NDVI, precipitation, NDRE, reservoir outflow, LAI, temperature, soil texture, relative humidity and EVI in influencing turmeric yield were 26.33%, 24.84%, 17.97%, 8.79%, 8.76%, 4.53%, 3.28%, 2.52%, 1.54% and 1.44%, respectively. The results revealed that MSI (26.33%), NDVI (24.84%) and precipitation (17.97%) had the highest influence, highlighting their direct relationship with water stress, vegetative vigor and moisture availability. NDRE (8.79%) and reservoir outflow (8.76%) had a moderate influence, supporting the role of canopy health and irrigation in yield formation. Other variables like LAI (4.53%), temperature (3.28%), soil texture (2.52%), relative humidity (1.54%) and EVI (1.44%) showed relatively lower sensitivity, suggesting that minor fluctuations in these inputs had limited impact on yield outcomes. These results underscore the importance of water-related and vegetation indices in accurately modelling turmeric yield and validate the model's responsiveness to biophysically relevant inputs.

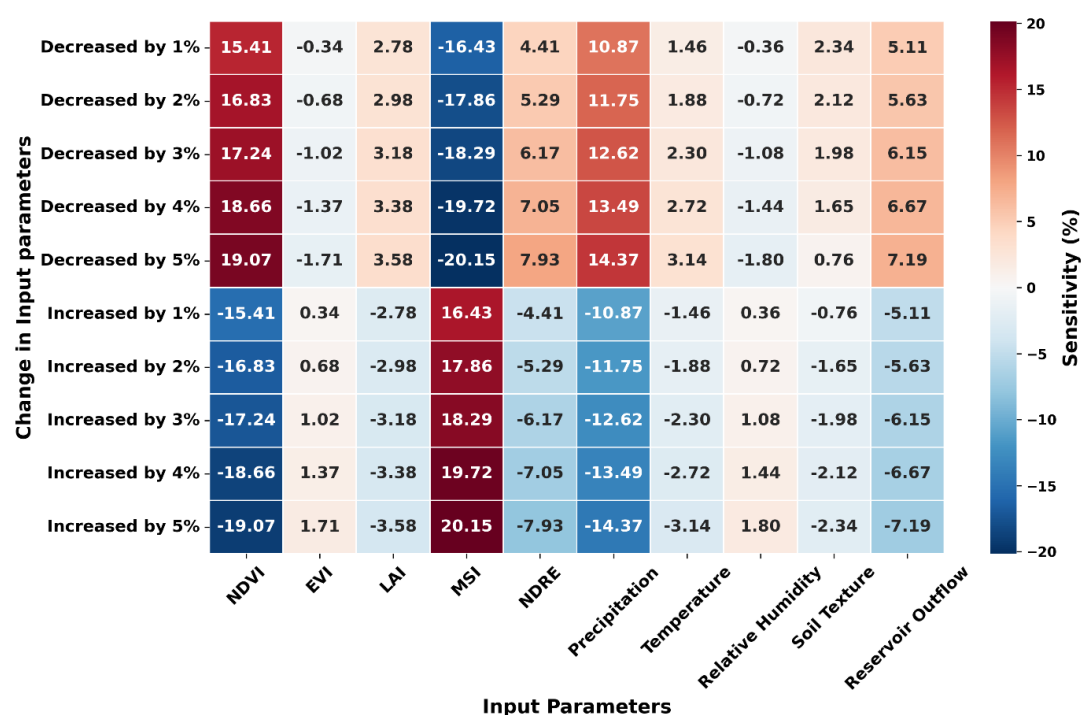
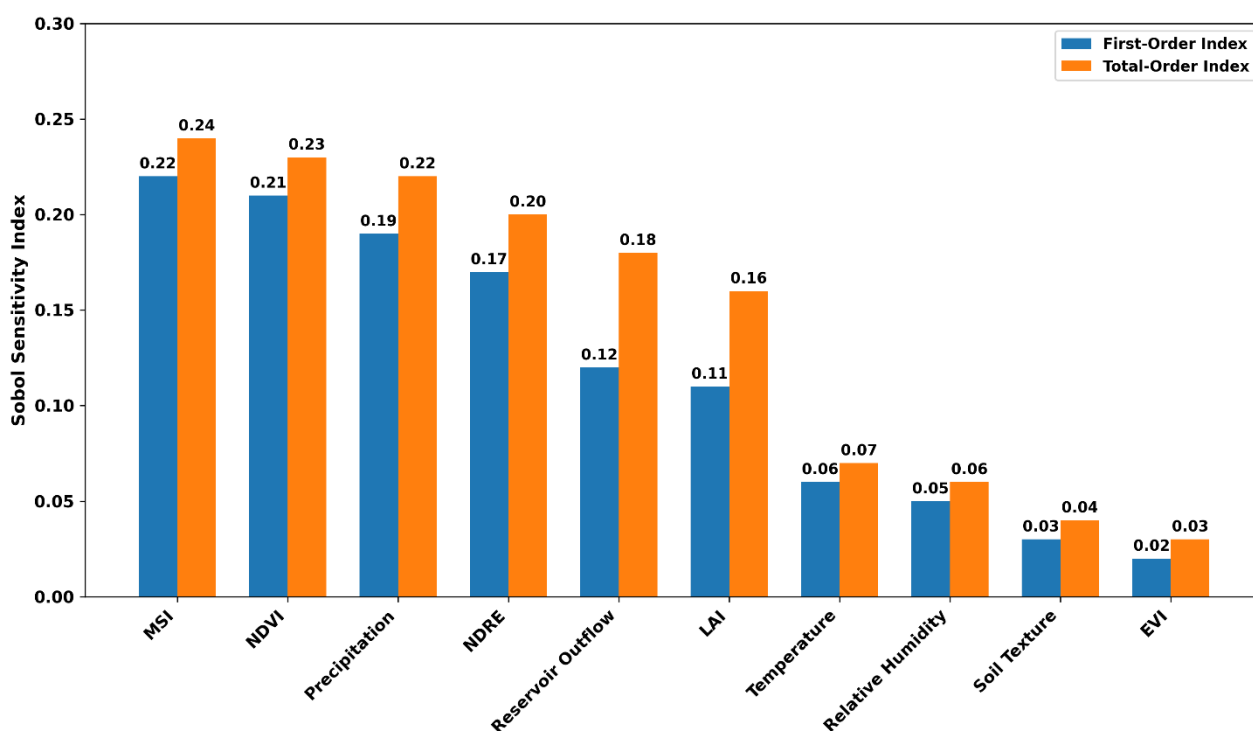


Figure 4 OAT Sensitivity analysis results for turmeric yield

In addition to the OAT sensitivity analysis, the Global Sensitivity Analysis (GSA) was conducted utilizing Sobol indices through the SALib Python package and the results are shown in **Error! Reference source not found..** The technique measures both individual (first-order) and interaction (total-order) impacts of input parameters on turmeric yield prediction. Identifying MSI (0.24), NDVI (0.23) and precipitation (0.22) as the dominant parameters, which had the maximum total-order indices were established, reflecting their leading contributions both through direct impact and through interaction. NDRE (0.20) and reservoir outflow (0.18) also yielded high total-order contributions, with LAI (0.16) and temperature (0.07) yielding moderate sensitivity. Parameters like relative humidity, soil texture and EVI had a lower overall impact. However, the greater difference between their total- and first-order indices indicated that their influence derives mostly from interactions. These results generally corresponded to the OAT results, with the added point of highlighting the value of global sensitivity methods in uncovering interactive effects among input variables that would otherwise be overlooked.



**Figure 5 Global Sensitivity Analysis results for turmeric yield**

This approach enhanced the robustness of the sensitivity interpretation by capturing both main and interaction effects across the parameter space. The consistency in the top variable rankings between the OAT and Sobol-based GSA supported the reliability of the originally adopted OAT approach, especially for identifying the primary drivers of model performance.

### 3.6 Spatial validation

The spatial validation of the BPNN model further underscores its reliability and adaptability across different regions. The model trained on data from Erode, Coimbatore and Tiruppur was tested on Salem and Dharmapuri, two agriculturally significant turmeric producing districts with distinct microclimatic and soil conditions. The model's predictive accuracy remained high, with  $R^2$  values of 0.91 in Salem and 0.89 in Dharmapuri, indicating a strong correlation between predicted and observed yields. The relatively low Root Mean

Squared Error (RMSE) values (0.31 t/ha and 0.36 t/ha, respectively) further highlighted the model's robustness in capturing yield variability in unseen regions. These findings validated the model's transferability across agro-climatic zones making it a promising tool for large-scale yield forecasting.

### 3.7 Future prediction

The BPNN model projections revealed distinct trends in turmeric yield under varying climate futures and are shown in **Error! Reference source not found.** SSP1-2.6 and SSP2-4.5 which assume lower greenhouse gas emissions and more sustainable trajectories, indicated relatively stable yield patterns with a slight increase toward the end of the century. The average predicted yield under these scenarios remained between 4.8 and 5.2 t/ha throughout the century, with modest fluctuations and narrower confidence intervals indicating more reliable and consistent rainfall patterns. SSP3-7.0 and SSP4-6.0 yield projections showed increased variability, particularly around mid-century, reflecting the effects of more erratic or regionally imbalanced rainfall distributions. Predicted yields under these scenarios occasionally dip below 4.8 t/ha, indicating the potential stress turmeric crops may face due to irregular precipitation. SSP5-8.5, the high-emission scenario resulted in the highest average projected yields (around 5.6 to 6.2 t/ha). However, the wide confidence bands suggested substantial uncertainty, potentially due to extreme rainfall events or anomalies under this fossil-fuelled development pathway.

Overall, the results highlighted that even when other biophysical and environmental conditions remain constant, variations in precipitation alone as shaped by different climate scenarios can significantly influence turmeric yield. This emphasized the need for rainfall-focused adaptation strategies, such as improved water management and irrigation infrastructure, to ensure yield stability under future climate conditions.

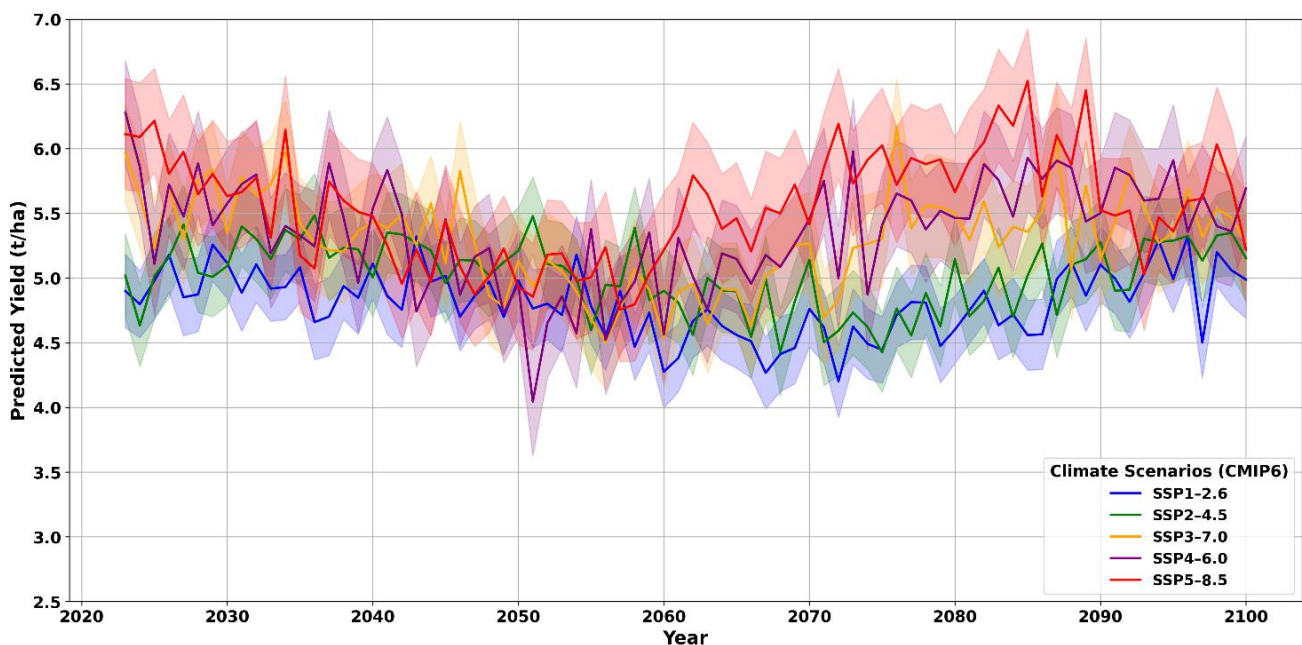


**Figure 6 Future projection of turmeric yield under SSP scenario**

Climate scenarios (SSPs) are alternative socio-economic and emission paths each influencing climatic factors like rainfall and temperature that are essential for growing turmeric. The application of multiple SSPs brings uncertainty into the projection of the future because they differ in assumed emissions and connected climate response. For instance, SSP1-2.6 and SSP2-4.5 under the assumption of sustainable development and moderate emissions respectively, have relatively narrow confidence intervals in projected yields, reflecting more stable and predictable rainfall and temperature patterns. On the other hand, SSP3-7.0 and SSP5-8.5 are marked by increased emissions and climatic volatility, leading to wider confidence intervals and higher uncertainty in projected yields. This heterogeneity emphasizes the need for incorporating uncertainty bands when analyzing model outputs.



522

### 523 3.8 Robustness Analysis under Severe Climatic Conditions

524 To assess the robustness of the model in years of extreme weather, a historical  
525 robustness analysis was conducted by distinguishing anomalous climatic years. Specifically,  
526 the years 2017 and 2019, which experienced record-breaking monthly rainfall (>450 mm) and  
527 2016 with record-breaking average temperature (>31°C) were employed for this analysis. The  
528 performance of the model was assessed once again using data from these extreme years. The  
529 results showed that the performance metrics ( $R^2 = 0.88$ , RMSE = 0.26 t/ha, Mean Absolute  
530 Error (MAE) = 0.07 t/ha) were at less than desirable levels justifying that the model was stable  
531 to atypical environmental conditions. The results confirmed that the model has robustness in  
532 the way that it can survive non-typical environmental inputs while still being able to function  
533 when predicting turmeric yield under actual climatic variation. In addition, the model also  
534 performed consistently well under these outlier years which warrants its validity and  
535 applicability to situations in the future.

536

### 537 3.9 Assessment of Model Performance in Predicting Crop Yield at Growth Stages

538 The turmeric crop yield was predicted with the data observed in each crop growth  
539 phase and the results are shown in **Error! Reference source not found..** The growth phases  
540 of turmeric include the emerging, vegetative, maturity and harvest phases.

541

#### 542 a. Emerging Phase

543 The predicted yield differed from the actual turmeric yield by 30.38 % in the emerging  
544 phase. This implied a relatively high uncertainty in all these predictions, especially during this  
545 early growth phase because of the extremely high sensitivity to environmental conditions.

Young turmeric plants are notably sensitive to environmental conditions, thus rendering it difficult to make accurate predictions.

#### **b. Vegetative Stage**

The predicted yield differed from the actual turmeric yield by 26.35 % in the vegetative stage. This signalled a great prediction error, although lower than the emerging phase of the most recent research on turmeric. More data will be available as the plant grows, but environmental and management-induced growth variability will always play a big role in prediction accuracy. This stage was characterized by vigorous development of the leaves, stems and biomass. During the vegetative stage, the plant directs its energies toward foliage improvement for better photosynthesis, which will facilitate rhizome development. The vegetative growth is highly dependent on light, water and nutrients. The disturbance in these factors brings a great deal of variability to the growth of each plant and yield, thereby discriminating against prediction.

#### **c. Maturity Phase**

In this phase, the predicted yield was much closer to the actual yield, with only a 1.23 % difference in turmeric yield. The prediction became more precise at the maturity stage, owing to a more stable pattern in plant growth and adequate data. During the maturity stage, the turmeric plant slows down vegetative growth while it starts the process of rhizome development and maturation. Canopy development is complete and energy is directed towards the swelling of rhizomes and starch accumulation. This is the stage when the growth rate of a plant becomes steady with some predictable growth in rhizomes and biomass. There was more consistency and accuracy in maturity-stage data such as leaf area, plant height and rhizome growth, which allowed for more precise predictions of yield. Mature plants are more resilient to environmental

stress. Hence, the impact of adverse conditions on growth is less disturbing than in earlier stages. This resilience was responsible for reducing variations in growth and thus increasing the accuracy of prediction.

#### **d. Harvest Phase**

The smallest difference was observed during the harvest phase, with a 1.23 % change from the actual turmeric yield. Although harvest phase estimates remained accurate, there was a modest increase in deviation compared to the maturity phase. This small difference was due to factors affecting the crop during the late season, such as weather fluctuations.

The results indicated the model's ability to forecast what the yield at maturity will finally be with minimum variance relative to the actual outcome right at the maturity stage, as opposed to the harvest stage. This gives early insights that help allocate resources, schedules for harvesting and market planning, culminating in practical benefits of earlier decision-making.

**Table 3 Turmeric crop yield prediction at different phases of growth**

<b>Growth Phase</b>	<b>Change in predicted yield from actual yield (%)</b>
<b>Emerging Phase</b>	30.38
<b>Vegetative Phase</b>	26.35
<b>Maturity Phase</b>	0.86
<b>Harvest Phase</b>	1.22

#### 588 4. Conclusions

589 Correlation analysis indicated that MSI, NDRE and rainfall were highly correlated with  
590 turmeric yield, highlighting the importance of water availability and plant health. The BPNN model  
591 had the highest accuracy ( $R^2 = 0.96$ ), which was higher than other models because of its ability to  
592 learn intricate patterns. This led to superior model performance, achieving the highest coefficient of  
593 determination ( $R^2$ ) and the lowest error metrics among all crop yield prediction models evaluated in  
594 this study. Sensitivity analysis validated MSI, NDVI and rainfall as the most significant variables.  
595 Phase-wise yield predictions showed that the BPNN model was able to accurately predict yield at  
596 the maturity phase with only a 0.86% difference, providing early information for harvest planning  
597 and resource allocation. This predictive model connects environmental factors to turmeric  
598 production and encourages climate-resilient farming. It aligns with Sustainable Development Goals  
599 (SDGs) 2 (Zero Hunger), 6 (Clean Water), 12 (Responsible Consumption) and 13 (Climate Action)  
600 by facilitating decision-making, optimizing resources and environmental protection. The use of  
601 remote sensing and machine learning in this research establishes its viability for scaling up  
602 sustainable agriculture solutions. Though the model was customized to turmeric, subsequent  
603 research must investigate adaptation to other crops and implement deep learning techniques for  
604 higher accuracy and resilience. Expanded usability necessitates reformulating inputs and parameters  
605 to accommodate various types of crops. Economic viability, user acceptability and policy  
606 embedding are critical to field-level implementation. Although this research did not incorporate  
607 cost-benefit and farmer feedback studies, spatial validation has confirmed the model's  
608 transferability, thereby establishing a foundation for future studies focusing on economic feasibility,  
609 user acceptance and policy integration. Future studies may involve a comparative assessment of  
610 sophisticated classification techniques like Random Forest (RF), Support Vector Machines (SVM)  
611 and deep learning-based methods, which are reported to provide better performance in sophisticated  
612 land cover classification applications. Optimization of MLC by using better training sample

selection, incorporation of ancillary data sets, or hybrid methods can also enhance classification accuracy to some degree.

## References

- Abrougui, K., Gabsi, K., Mercatoris, B., Khemis, C., Amami, R. and Chehaibi, S. (2019). Prediction of organic potato yield using tillage systems and soil properties by artificial neural network (ANN) and multiple linear regressions (MLR). *Soil and Tillage Research*, **190**, 202–208.
- Ahmad, I., Saeed, U., Fahad, M., Ullah, A., Habib ur Rahman, M., Ahmad, A. and Judge, J. (2018). Yield Forecasting of Spring Maize Using Remote Sensing and Crop Modeling in Faisalabad-Punjab Pakistan. *Journal of the Indian Society of Remote Sensing*, **46**, 1701–1711
- Akbar, A., Kuanar, A., Joshi, R. K., Sandeep, I. S., Mohanty, S., Naik, P. K., Mishra, A. and Nayak, S. (2016). Development of prediction model and experimental validation in predicting the curcumin content of turmeric (*Curcuma longa* L.). *Frontiers in Plant Science*, **7**, 1–17.
- Akbar, A., Kuanar, A., Patnaik, J., Mishra, A. and Nayak, S. (2018). Application of Artificial Neural Network modeling for optimization and prediction of essential oil yield in turmeric (*Curcuma longa* L.). *Computers and Electronics in Agriculture*, **148**, 160–178.
- Amankulova, K., Farmonov, N. and Mucsi, L. (2023). Time-series analysis of Sentinel-2 satellite images for sunflower yield estimation. *Smart Agricultural Technology*, **3**. Aslan, M. F., Sabanci, K., and Aslan, B. (2024). Artificial Intelligence Techniques in Crop Yield Estimation Based on Sentinel-2 Data: A Comprehensive Survey. In *Sustainability* **16**..
- Bali, N. and Singla, A. (2021). Deep Learning Based Wheat Crop Yield Prediction Model in Punjab Region of North India. *Applied Artificial Intelligence*, **35**, 1304–1328.
- Bassine, F. Z., Epule, T. E., Kechchour, A. and Chehbouni, A. (2023). Recent applications of machine learning, remote sensing and iot approaches in yield prediction: a critical review.
- Bharadiya, J. P., Tzenios, N. T. and Reddy, M. (2023). Predicting Crop Yield Using Deep Learning and Remote Sensing. *Journal of Engineering Research and Reports*, **24**, 29–44.
- Bulacio Fischer, P. T., Carella, A., Massenti, R., Fadhilah, R. and Lo Bianco, R. (2025). Advances in Monitoring Crop and Soil Nutrient Status: Proximal and Remote Sensing Techniques. *Horticulturae* **11**.
- Das, B., Nair, B., Reddy, V. K. and Venkatesh, P. (2018). Evaluation of multiple linear, neural network and penalised regression models for prediction of rice yield based on weather parameters for west coast of India. *International Journal of Biometeorology*, **62**, 1809–1822.
- Dharwadkar, N. V, Kalmani, V. H. and Thapa, V. (2023). *Crop yield prediction using deep learning algorithm based on CNN-LSTM with Attention Layer and Skip Connection*. Dimov, D., Uhl, J. H., Löw, F., and Seboka, G. N. (2022). Sugarcane yield estimation through remote sensing time series and phenology metrics. *Smart Agricultural Technology*, **2**.
- El-Kenawy, E.-S. M., Alhussan, A. A., Khodadadi, N., Mirjalili, S. and Eid, M. M. (2025). Predicting Potato Crop Yield with Machine Learning and Deep Learning for Sustainable Agriculture. *Potato Research*, **68**, 759–792

651 Goodfellow, I., Bengio, Y. and Courville, A. (n.d.). (2016), *Deep Learning*, MIT Press.

652 Hara, P., Piekutowska, M. and Niedbała, G. (2021). Selection of independent variables for crop yield  
653 prediction using artificial neural network models with remote sensing data. *Land*, **10**(6).

654 Huber, F., Inderka, A. and Steinhage, V. (2024). Leveraging Remote Sensing Data for Yield Prediction  
655 with Deep Transfer Learning. *Sensors (Basel, Switzerland)*, **24**, 770.

656 Hunt, M. L., Blackburn, G. A., Carrasco, L., Redhead, J. W. and Rowland, C. S. (2019). High  
657 resolution wheat yield mapping using Sentinel-2. *Remote Sensing of Environment*, **233**.

658 Ishaq, R. A. F., Zhou, G., Tian, C., Tan, Y., Jing, G., Jiang, H. and Obaid-ur-Rehman. (2024). A  
659 Systematic Review of Radiative Transfer Models for Crop Yield Prediction and Crop Traits  
660 Retrieval. *Remote Sensing*, **16**.

661 Ji, Z., Pan, Y., Zhu, X., Wang, J. and Li, Q. (2021). Prediction of Crop Yield Using Phenological  
662 Information Extracted from Remote Sensing Vegetation Index. *Sensors*, **21**, 1406.

663 Johnson, D. M. (2014). An assessment of pre- and within-season remotely sensed variables for  
664 forecasting corn and soybean yields in the United States. *Remote Sensing of Environment*, **141**,  
665 116–128. Joshi, A., Pradhan, B., Gite, S., and Chakraborty, S. (2023). Remote-Sensing Data and  
666 Deep-Learning Techniques in Crop Mapping and Yield Prediction: A Systematic Review.  
667 *Remote Sensing*, **15**.

668 Joshua, V., Priyadharson, S. M. and Kannadasan, R. (2021). Exploration of machine learning  
669 approaches for paddy yield prediction in eastern part of Tamilnadu. *Agronomy*, **11**. Kavipriya,  
670 J., and Vadivu, G. (2024). Exploring Crop Yield Prediction with Remote Sensing Imagery and  
671 AI. *Proceedings - 3rd International Conference on Advances in Computing, Communication and*  
672 *Applied Informatics*,

673 Khaki, S. and Wang, L. (2019). Crop yield prediction using deep neural networks. *Frontiers in Plant*  
674 *Science*, **10**, 452963. Li, M., Sun, H., and Zhao, R. (2023). A Review of Root Zone Soil Moisture  
675 Estimation Methods Based on Remote Sensing. *Remote Sensing*, **15**,

676 Lin, F., Crawford, S., Guillot, K., Zhang, Y., Chen, Y., Yuan, X., Chen, L., Williams, S., Minvielle,  
677 R., Xiao, X., Gholson, D., Ashwell, N., Setiyono, T., Tubana, B., Peng, L., Bayoumi, M. and  
678 Tzeng, N.-F. (2023). *MMST-ViT: Climate Change-aware Crop Yield Prediction via Multi-Modal*  
679 *Spatial-Temporal Vision Transformer. Proceedings of the IEEE International Conference on*  
680 *Computer Vision*, 5751-5761.

681 Mateo-Sanchis, A., Piles, M., Muñoz-Marí, J., Adsuaara, J. E., Pérez-Suay, A. and Camps-Valls, G.  
682 (2020). Synergistic Integration of Optical and Microwave Satellite Data for Crop Yield  
683 Estimation. *Remote Sensing of Environment*, **234**.

684 Mena, F., Pathak, D., Najjar, H., Sanchez, C., Helber, P., Bischke, B., Habelitz, P., Miranda, M.,  
685 Siddamsetty, J., Nuske, M., Charfuelan, M., Arenas, D., Vollmer, M. and Dengel, A. (2024).  
686 *Adaptive Fusion of Multi-view Remote Sensing data for Optimal Sub-field Crop Yield*  
687 *Prediction*. **318**, 114547.

688 Moussa Kourouma, J., Eze, E., Negash, E., Phiri, D., Vinya, R., Girma, A. and Zenebe, A. (2021).  
689 Assessing the spatio-temporal variability of NDVI and VCI as indices of crops productivity in  
690 Ethiopia: a remote sensing approach. *Geomatics, Natural Hazards and Risk*, **12**, 2880–2903.

691 Muruganantham, P., Wibowo, S., Grandhi, S., Samrat, N. H. and Islam, N. (2022). A Systematic  
692 Literature Review on Crop Yield Prediction with Deep Learning and Remote Sensing. *Remote*  
693 *Sensing* , **14**, 1990.

694 Mwaura, J. I. and Kenduiywo, B. K. (2021). County level maize yield estimation using artificial  
695 neural network. In *Modeling Earth Systems and Environment* 71417–1424.

696 Nevavuori, P., Narra, N. and Lipping, T. (2019). Crop yield prediction with deep convolutional neural  
697 networks. *Computers and Electronics in Agriculture*, **163**.

698 Potopová, V., Trnka, M., Hamouz, P., Soukup, J. and Castraveţ, T. (2020). Statistical modelling of  
699 drought-related yield losses using soil moisture-vegetation remote sensing and multiscalar  
700 indices in the south-eastern Europe. *Agricultural Water Management*, **236**.

701 Raju, A. M., Tom, M., Karadi, N. P. and Subramani, S. (2023). Spice Yield Prediction for Sustainable  
702 Food Production Using Neural Networks. *Lecture Notes on Data Engineering and*  
703 *Communications Technologies*, **131**, 425–440.

704 Resop, J. P., Fleisher, D. H., Wang, Q., Timlin, D. J. and Reddy, V. R. (2012). Combining explanatory  
705 crop models with geospatial data for regional analyses of crop yield using field-scale modeling  
706 units. *Computers and Electronics in Agriculture*, **89**, 51–61.

707 Rojas, O., Vrieling, A. and Rembold, F. (2011). Assessing drought probability for agricultural areas  
708 in Africa with coarse resolution remote sensing imagery. *Remote Sensing of Environment*,  
709 **115**(2), 343–352.

710 Ronchetti, G., Manfron, G., Weissteiner, C. J., Seguí, L., Nisini Scacchiafichi, L., Panarello, L. and  
711 Baruth, B. (2023). Remote sensing crop group-specific indicators to support regional yield  
712 forecasting in Europe. *Computers and Electronics in Agriculture*, **205**, 107633.

713 Sajid, S. S., Shahhosseini, M., Huber, I., Hu, G. and Archontoulis, S. V. (2022). County-scale crop  
714 yield prediction by integrating crop simulation with machine learning models. *Frontiers in Plant*  
715 *Science*, **13**, 1000224.

716 Schmidt, M. and Felsche, E. (2024). The effect of climate change on crop yield anomaly in Europe.  
717 *Climate Resilience and Sustainability*, **3**.

718 Schwalbert, R. A., Amado, T. J. C., Nieto, L., Varela, S., Corassa, G. M., Horbe, T. A. N., Rice, C.  
719 W., Peralta, N. R. and Ciampitti, I. A. (2018). Forecasting maize yield at field scale based on  
720 high-resolution satellite imagery. *Biosystems Engineering*, **171**, 179–192.

721 Setiyono, T. D., Quicho, E. D., Gatti, L., Campos-Taberner, M., Busetto, L., Collivignarelli, F.,  
722 García-Haro, F. J., Boschetti, M., Khan, N. I. and Holecz, F. (2018). Spatial rice yield estimation  
723 based on MODIS and Sentinel-1 SAR data and ORYZA crop growth model. *Remote Sensing*,  
724 **10**.

725 Singh, P., Borgohain, S. K., Sarkar, A. K., Kumar, J. and Sharma, L. D. (2023). Feed-Forward Deep  
726 Neural Network (FFDNN)-Based Deep Features for Static Malware Detection. *International*  
727 *Journal of Intelligent Systems*, **1**, 1-20.

728 Srivastava, N., Hinton, G., Krizhevsky, A. and Salakhutdinov, R. (2014). Dropout: A Simple Way to  
729 Prevent Neural Networks from Overfitting. *Journal of Machine Learning Research*, **15**.

730 Sun, J., Di, L., Sun, Z., Shen, Y. and Lai, Z. (2019). County-level soybean yield prediction using deep  
731 CNN-LSTM model. *Sensors*, **19**, 1–21.

- 732 Tang, X., Liu, H., Feng, D., Zhang, W., Chang, J., Li, L. and Yang, L. (2022). Prediction of field  
733 winter wheat yield using fewer parameters at middle growth stage by linear regression and the  
734 BP neural network method. *European Journal of Agronomy*, **141**, 126621.
- 735 Tedesco, D., de Oliveira, M. F., dos Santos, A. F., Costa Silva, E. H., de Souza Rolim, G. and da Silva,  
736 R. P. (2021). Use of remote sensing to characterize the phenological development and to predict  
737 sweet potato yield in two growing seasons. *European Journal of Agronomy*, **129**.
- 738 *THE 17 GOALS | Sustainable Development*. (n.d.). Retrieved January 7, 2025, from  
739 <https://sdgs.un.org/goals>
- 740 Xu, Q., Liang, H., Wei, Z., Zhang, Y., Lu, X., Li, F., Wei, N., Zhang, S., Yuan, H., Liu, S. and Dai, Y.  
741 (2024). Assessing Climate Change Impacts on Crop Yields and Exploring Adaptation Strategies  
742 in Northeast China. *Earth's Future*, **12**.
- 743 Yang, G., Jin, N., Ai, W., Zheng, Z., He, Y. and He, Y. (n.d.). (2025). Integrating remote sensing data  
744 assimilation, deep learning and large language model for interactive wheat breeding yield  
745 prediction. Cornell University
- 746 Yeşilköy, S. and Demir, I. (2024). Crop yield prediction based on reanalysis and crop phenology data  
747 in the agroclimatic zones. *Theoretical and Applied Climatology*, **155**, 7035–7048.
- 748 Zhou, X., Zheng, H. B., Xu, X. Q., He, J. Y., Ge, X. K., Yao, X., Cheng, T., Zhu, Y., Cao, W. X. and  
749 Tian, Y. C. (2017). Predicting grain yield in rice using multi-temporal vegetation indices from UAV-  
750 based multispectral and digital imagery. *ISPRS Journal of Photogrammetry and Remote Sensing*, **130**,  
751 246–255.

## 752 **Funding**

753 This research did not receive any specific grant from funding agencies in the public, commercial, or  
754 not-for-profit sectors.

## 755 **Declaration of competing interest**

756 We affirm no conflicts of interest in this research article.

## 757 **Acknowledgements**

758 We extend our sincere gratitude to the reviewers for their insightful comments and valuable  
759 contributions, which have greatly enhanced the manuscript.

760

761

762



763 **List of Figures**

764 **Error! Reference source not found.**

765 **Error! Reference source not found.**

766 **Error! Reference source not found.**

767 **Error! Reference source not found.**

768 **Error! Reference source not found.**

769 **Error! Reference source not found.**

770 **List of Tables**

771 **Error! Reference source not found.**

772 **Error! Reference source not found.**

773 **Error! Reference source not found. Error! Reference source not found.**

774